Activation of the calcium-sensing receptor induces deposition of tight junction components to the epithelial cell plasma membrane

François Jouret[1,2], Jingshing Wu[1], Michael Hull[1], Vanathy Rajendran[1], Bernhard Mayr[3], Christof Schöfl[2], John Geibel[1] and Michael J. Caplan[1,*]

[1]Department of Cellular and Molecular Physiology, Yale School of Medicine, New Haven, CT 06520, USA
[2]University of Liege Hospital (ULg CHU), Division of Nephrology and GIGA Cardiovascular Sciences, 4000 Liège, Belgium
[3]Division of Endocrinology and Diabetes, Department of Medicine I, Friedrich-Alexander University Erlangen-Nuremberg, 91054 Erlangen, Germany
*Author for correspondence (michael.caplan@yale.edu)

Accepted 27 August 2013
Journal of Cell Science 000, 1–12

doi: 10.1242/jcs.127555

Summary

The calcium-sensing receptor (CaSR) belongs to the G-protein-coupled receptor superfamily and plays essential roles in divalent ion homeostasis and cell differentiation. Because extracellular Ca^{2+} is essential for the development of stable epithelial tight junctions (TJs), we hypothesized that the CaSR participates in regulating TJ assembly. We first assessed the expression of the CaSR in Madin-Darby canine kidney (MDCK) cells at steady state and following manipulations that modulate TJ assembly. Next, we examined the effects of CaSR agonists and antagonists on TJ assembly. Immunofluorescence studies indicate that endogenous CaSR is located at the basolateral pole of MDCK cells. Stable transfection of human CaSR in MDCK cells further reveals that this protein co-distributes with β-catenin on the basolateral membrane. Switching MDCK cells from low-Ca^{2+} medium to medium containing a normal Ca^{2+} concentration significantly increases CaSR expression at both the mRNA and protein levels. Exposure of MDCK cells maintained in low-Ca^{2+} conditions to the CaSR agonists neomycin, Gd^{3+} or R-568 causes the transient relocation of the tight junction components ZO-1 and occludin to sites of cell–cell contact, while inducing no significant changes in the expression of mRNAs encoding junction-associated proteins. Stimulation of CaSR also increases the interaction between ZO-1 and the F-actin-binding protein I-afadin. This effect does not involve activation of the AMP-activated protein kinase. By contrast, CaSR inhibition by NPS-2143 significantly decreases interaction of ZO-1 with I-afadin and reduces deposition of ZO-1 at the cell surface following a Ca^{2+} switch from 5 μM to 200 μM $[Ca^{2+}]_e$. Pre-exposure of MDCK cells to the cell-permeant Ca^{2+} chelator BAPTA-AM, similarly prevents TJ assembly caused by CaSR activation. Finally, stable transfection of MDCK cells with a cDNA encoding a human disease-associated gain-of-function mutant form of the CaSR increases the transepithelial electrical resistance of these cells in comparison to expression of the wild-type human CaSR. These observations suggest that the CaSR participates in regulating TJ assembly.

Key words: Calcium-sensing receptor, Epithelia, Tight junction

Introduction

The Ca^{2+}-sensing receptor (CaSR) belongs to family C of the G-protein-coupled receptor (GPCR) superfamily (Brown et al., 1993; Bräuner-Osborne et al., 2007). The CaSR is ubiquitously expressed and consists of an extracellular domain, a seven-transmembrane domain and an intracellular loop. Its principal physiological ligand is the Ca^{2+} ion. By sensing minute variations of the extracellular Ca^{2+} concentration ($[Ca^{2+}]_e$) and appropriately modulating the cellular responses to these changes, the CaSR plays an essential role in Ca^{2+} homeostasis. Hence, it controls parathyroid hormone (PTH) secretion by the parathyroid glands and modulates Ca^{2+} fluxes in the kidney and the bone (Chakravarti et al., 2012; Geibel, 2010). Mutations in the *CASR* gene have been associated with inherited disorders of divalent mineral homeostasis (Pearce, et al., 1996; Hannan et al., 2012). Loss-of-function mutations in one or both of the *CASR* alleles result in hypercalcemic disorders as a result of upward resetting of the receptor EC_{50} value (effective concentration necessary to induce a 50% effect) for ionized Ca^{2+} in both the parathyroid glands and the kidney (Gunn and Gaffney, 2004; Thakker, 2004; Rus et al., 2008). Conversely, gain-of-function mutations of the *CASR* gene result in hypocalcemia because of downward resetting of the receptor EC_{50} (Chattopadhyay and Brown, 2006; Letz et al., 2010). Furthermore, the EC_{50} value for Ca^{2+} binding to the CaSR can be significantly affected by several physiological parameters, including ionic strength, extracellular pH, L-aromatic amino acids and polyamines, or by drugs, such as the calcimimetic compounds cinacalcet HCl and R-568. In addition, the CaSR can be directly activated by many di-, tri- and polyvalent cations, including neomycin and Gd^{3+}, in the absence of extracellular Ca^{2+} (Nemeth, 2004).

Interestingly, the CaSR has been identified in numerous tissues and cells that are not directly involved in Ca^{2+} homeostasis, in which its role remains unclear (Magno et al., 2011; Riccardi and Kemp, 2012). All along the gastro-intestinal tract, the CaSR participates in nutrient sensing, hormone and fluid secretion, and cell differentiation and apoptosis (Gama et al., 1997). In the skin, the CaSR has been shown to regulate cell survival and Ca^{2+}-induced differentiation of epidermal keratinocytes (Komuves

et al., 2002; Fatherazi et al., 2004; Troy et al., 2007; Tu et al., 2008). Differentiated epithelial cells possess highly specialized intercellular junctions, including adherens junctions (AJs) and tight junctions (TJs). TJs form a seal at the superior aspect of the lateral surface of the plasma membrane when epithelial cells differentiate and acquire polarity. TJs regulate the passage of ions and small molecules through the paracellular pathway (Van Itallie and Anderson, 2004), and also restrict the diffusion of membrane proteins between the apical and basolateral compartments (van Meer and Simons, 1986). Extracellular Ca^{2+} is essential for both the development of new junctions (Cereijido et al., 1981; Gonzalez-Mariscal et al., 1985; Martinez-Palomo et al., 1980) and the stabilization of mature junctions (Galli et al., 1976; Hays et al., 1965; Meldolesi et al., 1978; Palant et al., 1983; Sedar and Forte, 1964) between epithelial cells. The dependence of TJ assembly on Ca^{2+} is probably attributable to the capacity of Ca^{2+} to stabilize the cell adhesion molecule E-cadherin in its adhesive state at AJs (Boller et al., 1985; Ringwald et al., 1987). However, recent observations demonstrated that the CaSR regulates the expression of TJ components, including claudins, in kidney epithelial cells (Ikari et al., 2008; Gong et al., 2012). It is therefore tempting to speculate that the CaSR might also be implicated in regulating the Ca^{2+}-induced assembly of TJs in epithelial cells.

In the Madin-Darby canine kidney (MDCK) epithelial cell model, incubation in medium containing a reduced concentration of calcium (low $[Ca^{2+}]_e$) disrupts intercellular junctions, and the restoration of high $[Ca^{2+}]_e$ induces the deposition of TJ proteins to the plasma membrane. This manipulation is referred to as a 'Ca^{2+} switch', and is associated with a rise of the cytosolic concentration of Ca^{2+} (Cereijido et al., 1978; Gonzalez-Mariscal et al., 1990). Previous observations from our group and others have demonstrated that the Ca^{2+} switch stimulates various independent cellular cascades, including the protein kinase C (PKC), the AMP-activated protein kinase (AMPK) and the glycogen synthase kinase 3β (GSK-3β) pathways (Balda et al., 1991; Zhang et al., 2006; Zheng and Cantley, 2007; Zhang et al., 2011). In MDCK cells, a Ca^{2+} switch is typically associated with the activation of AMPK and the inhibition of GSK-3β. Activated AMPK phosphorylates I-afadin, at AJ sites, thereby inducing its interaction with and the recruitment of the TJ-associated protein ZO-1 to the plasma membrane. By contrast, I-afadin appears not to be required for the assembly of TJs caused by GSK-3β inhibition (Zhang et al., 2011).

Here, we show that the activation of the CaSR in MDCK cells by well-established agonists causes the relocation of TJ components to the plasma membrane. This CaSR-induced assembly of TJs is associated with an increased interaction between I-afadin and ZO-1, can be blocked by CaSR antagonists and occurs without the activation of AMPK. Pre-exposure of MDCK cells to the cell-permeant Ca^{2+} chelator, BAPTA-AM, prevents the relocation of TJ components after stimulation of the CaSR, but has no effect on TJ assembly induced by AMPK activation. These observations further support the concept that multiple independent pathways are implicated in the Ca^{2+}-induced formation of TJs in epithelial cells, and that one of these pathways involves the CaSR.

Results

Expression and distribution of the Ca^{2+}-sensing receptor in MDCK cells at steady state and after Ca^{2+} switch

The CaSR is found in various segments of the mammalian nephron, including the proximal tubule (PT), the thick ascending limb (TAL) of Henlé's loop, the distal tubule, and in both principal and intercalated cells of the collecting duct (CD) (Riccardi and Brown, 2010). Its subcellular distribution appears to be segment specific, manifesting an apical polarization in PT and CD cells, and a basolateral localization in TAL cells. The subcellular distribution of the CaSR in MDCK cells has yet to be determined. We performed co-immunofluorescence experiments on MDCK cells at steady state using antibodies directed against the CaSR and a marker of the basolateral membrane, β-catenin. We found that the endogenous CaSR is expressed in intracellular compartments and at the basolateral pole of MDCK cells (Fig. 1A).

MDCK cells represent a well-established model in which to study epithelial TJ formation, and junction formation can be temporally controlled using the Ca^{2+} switch (Cereijido et al., 1978). We cultured MDCK cells to confluence in high-Ca^{2+} medium (HCM, 1.8 mM $[Ca^{2+}]_e$) and then incubated them in low-Ca^{2+} medium (LCM, 5 μM Ca^{2+}) for 16 hours. At successive time points after the reintroduction of HCM, cells were lysed and analyzed. Real-time reverse transcription polymerase chain reaction (RT-PCR) and immunoblotting analyses showed that Ca^{2+} switch is associated with an increased expression of CaSR at both the mRNA and the protein levels (Fig. 1B–D). These observations suggest that the expression of the CaSR is induced by the Ca^{2+} switch.

Activation of the CaSR induces Ca^{2+}-independent deposition of junction components

Distinct types of CaSR agonists have been identified and categorized based upon their mode of action. Type I agonists directly activate the CaSR and include the divalent ion Ca^{2+}, as well as other multivalent cations. Type II agonists act as allosteric modifiers of Ca^{2+} affinity, and therefore require the presence of extracellular Ca^{2+} to properly activate the CaSR. We used both type I (neomycin and Gd^{3+}) and type-II (calcimimetic compound, R-568) agonists of the CaSR to investigate the putative role of the CaSR in TJ regulation and biogenesis. First, confluent MDCK cells at steady state were exposed to the compound R-568 (800 nM) or to neomycin (1 mM) diluted in normal-Ca^{2+} medium (1.8 mM $[Ca^{2+}]_e$) for 4 hours. Under these conditions, the transepithelial electrical resistance (TEER) increased to 570.8±23.9 ohm.cm^2 and 762.8±69.8 ohm.cm^2, respectively. These values were significantly higher than the TEER measured in MDCK cells exposed for 4 hours to DMSO (417.7±21.1 ohm.cm^2) or PBS (433.3±16.4 ohm.cm^2).

Next, confluent MDCK cells were exposed to LCM for 16 hours, and then incubated in LCM containing either neomycin (1 mM) or Gd^{3+} (100 μM) for 1 or 2 hours. We found that ZO-1 was significantly relocated to the sites of cell–cell contact after exposure to neomycin or Gd^{3+}, even in the virtual absence of extracellular Ca^{2+} (Fig. 2A,B). We observed fragmentary strands of ZO-1 on plasma membranes after as little as 1 hour of incubation with neomycin or Gd^{3+}. Exposure of MDCK cells to R-568 (800 nM) or neomycin (1 mM) for 4 hours under low-Ca^{2+} conditions (5 μM $[Ca^{2+}]_e$) did not induce a measurable TEER. Furthermore, the ZO-1 strands failed to become more consolidated and morphologically organized with prolonged treatment, and disappeared at 8 hours of continued exposure (Fig. 2A,B). A very similar pattern was observed when we used antibodies directed against occludin to assess the subcellular

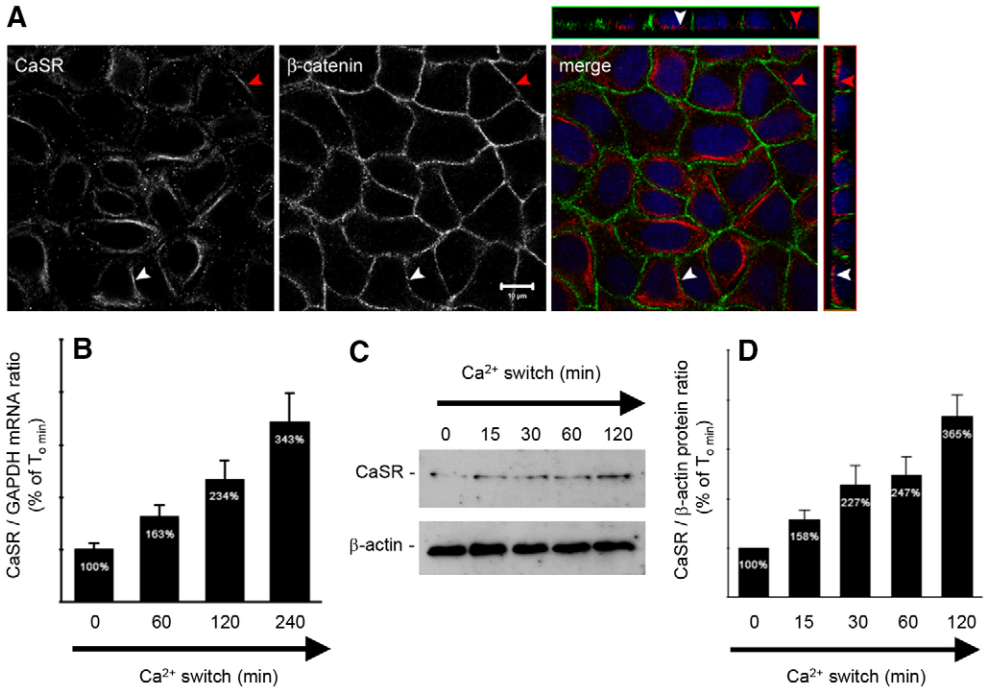

Fig. 1. Expression of the CaSR in MDCK cells at steady-state and following Ca^{2+} switch. (A) Representative co-immunofluorescence using rabbit polyclonal antibodies directed against the CaSR and mouse monoclonal antibodies directed against β-catenin, a marker of the basolateral membrane, in confluent MDCK cells. Merge panels show the *xyz* planes, with the CaSR labeled in red and β-catenin in green. Arrowheads indicate the basolateral side. Scale bar: 10 µm. (B–D) Comparative quantification of mRNA (B) and protein (C,D) expression of the CaSR in MDCK cells following Ca^{2+} switch. MDCK cells were lysed and processed at the indicated times after Ca^{2+} switch. Real-time RT-PCR was performed using specific primers directed against canine CaSR (target gene) and canine GAPDH (housekeeping gene), and the quantification was performed using the MxPro QPCR software (Stratagene). Immunoblotting quantification was performed using ImageJ software after normalization to β-actin expression levels. Data represent means ± s.d.

distribution of this essential transmembrane component of TJs in response to CaSR activation (supplementary material Fig. S1).

Finally, confluent MDCK cells were exposed to LCM for 16 hours and then incubated for 2 hours in LCM supplemented with either 50 µM or 200 µM $CaCl_2$ in the presence of vehicle alone (DMSO, DMSO), the CaSR antagonist NPS-2143 (1 µM) or the type II CaSR agonist R-568 (800 nM) (Fig. 3A,B). Switching MDCK cells from LCM to 50 µM $[Ca^{2+}]_e$ in the presence of DMSO was associated with relocation of ZO-1 to cell–cell contact sites. The magnitude of this process was significantly enhanced in the presence of R-568, but was not influenced by exposure to NPS-2143 (Fig. 3A,B). Similarly, switching MDCK cells from LCM to 200 µM $[Ca^{2+}]_e$ in the presence of DMSO induced a relocation of ZO-1 to the plasma membrane, which could be further increased in the presence of R-568. Interestingly, the quantity of ZO-1 relocation to MDCK cell–cell contacts following exposure to 200 µM $[Ca^{2+}]_e$ for 2 hours in the presence of NPS-2143 only reached the level observed after switching cells from LCM to 50 µM $[Ca^{2+}]_e$.

Altogether, these observations support the conclusion that the activation of the CaSR participates in the relocation of TJ components to cell–cell contacts. To further explore whether the pharmacological activation of the CaSR also influences the expression of TJ-associated proteins, we performed real-time RT-PCR on samples from MDCK cells maintained in low-Ca^{2+} conditions for 16 hours and then exposed for 4 hours to R-568 (800 nM) or neomycin (1 mM). We did not observe any major changes in expression of the mRNAs encoding type 1, 2 and 4 claudins or occludin in MDCK cells exposed to the CaSR agonists in comparison to control cells. The fact that the CaSR inhibitor only manifested effects on the ZO-1 relocation initiated by exposure to 200 µM but not to 50 µM $[Ca^{2+}]_e$, suggests that the Ca^{2+}-induced relocation of TJ components to the plasma membrane involves multiple mechanistically distinct Ca^{2+}-sensitive pathways with different Ca^{2+} affinities.

Activation of the CaSR in MDCK cells is not associated with the phosphorylation of AMPK, but increases the interaction between ZO-1 and l-afadin

Studies performed by our group and others have shown that a Ca^{2+} switch induces the phosphorylation and activation of AMPK in MDCK cells (Zhang et al., 2006; Zheng and Cantley, 2007). Conversely, the pharmacological activation of AMPK by AICAR induces Ca^{2+}-independent deposition of junction components to the sites of cell–cell contacts. Furthermore, both Ca^{2+} switch and AMPK activation increase the physical interaction between ZO-1 and l-afadin, a peripheral membrane protein located at the AJ that participates in organizing intercellular adhesive junctions (Ooshio et al., 2010; Zhang et al., 2011). Therefore, we assessed whether the relocation of ZO-1 to the plasma membrane following the activation of the CaSR involved the AMPK pathway. As in the previous experiment, confluent MDCK cells were exposed to LCM for 16 hours and then incubated in HCM or in LCM containing the type I CaSR agonists neomycin (1 mM) or Gd^{3+} (100 µM) for 30–60 minutes. Cells were lysed in the presence of protease and phosphatase inhibitors and processed for immunoblotting analysis. As previously described, Ca^{2+} switch induced a fourfold increase in AMPK T172 phosphorylation and AMPK activity, as reflected in the extent of S79 phosphorylation of acetyl CoA carboxylase (ACC) (Hardie and Pan, 2002) (Fig. 4A,B). By contrast, exposure to neomycin or Gd^{3+} was not associated with phosphorylation or activation of AMPK (Fig. 4A,B). The total amount of AMPKα1 catalytic subunit was not affected by any of the conditions tested. To further investigate the simultaneous processes implicated in relocation of TJ components following exposure to Ca^{2+}, we incubated confluent MDCK cells that had been initially kept for 16 hours in LCM in increasing concentrations of $CaCl_2$ in the presence of DMSO or R-568 for 30 minutes. Interestingly, we found that AMPK was phosphorylated and activated in MDCK cells following a Ca^{2+}

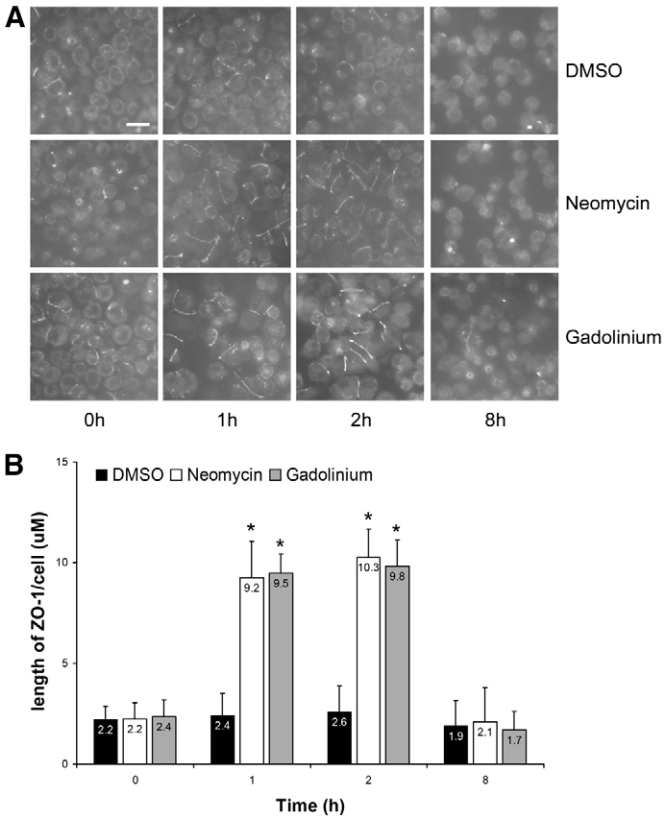

Fig. 2. Deposition of ZO-1 at the plasma membrane following activation of the CaSR in MDCK cells. (A) Confluent MDCK cells were incubated in low-Ca^{2+} medium (LCM) for 16 hours, exposed to fresh LCM supplemented with DMSO or with the CaSR agonists neomycin (1 mM) or Gd^{3+} (100 µM) for the indicated time points, fixed in ice-cold methanol, and immunostained for ZO-1. Scale bar: 50 µm. (B) Quantification of ZO-1 relocation to the cell membrane in A. Data represent means ± s.d., and are representative of four independent experiments. ZO-1 length per cell is measured within each of six randomly selected fields of view. *$P \leq 0.05$ versus incubation with DMSO by Student's *t*-test.

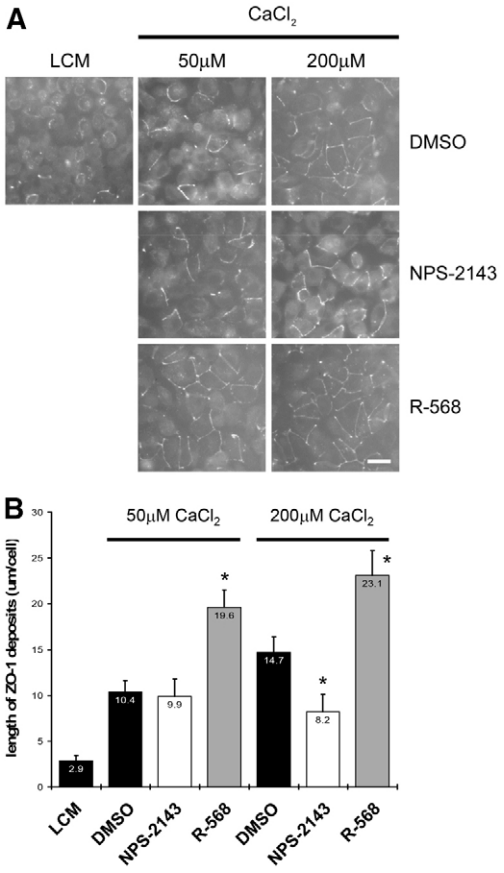

Fig. 3. Deposition of ZO-1 at the plasma membrane after modulation of the CaSR by R-568 in MDCK cells. (A) Confluent MDCK cells were incubated in low-Ca^{2+} medium (LCM) for 16 hours, exposed to fresh LCM supplemented with 50 µM or 200 µM $CaCl_2$ and DMSO, the CaSR antagonist NPS-2143 (1 µM) or the CaSR agonist R-568 (800 nM) for 2 hours, fixed in ice-cold methanol and immunostained for ZO-1. Scale bar: 50 µm. (B) Quantification of ZO-1 relocation to cell membrane in A. Data are means ± s.d., and are representative of four independent experiments. ZO-1 length per cell is measured within each of six randomly selected fields of view. *$P \leq 0.05$ versus incubation with DMSO by Student's *t*-test.

switch to concentrations as low as 50 µM (Fig. 4C,D). The level of AMPK phosphorylation was similar when the $[Ca^{2+}]_e$ was switched from 5 µM to 50 µM, 100 µM or 200 µM. Activation of the CaSR by R-568 did not modify the level of AMPK phosphorylation and activation induced by the exposure to any of these $[Ca^{2+}]_e$ values.

In MDCK cells, the formation of TJs requires the transient interaction of ZO-1 with I-afadin at the sites of initial cell–cell adhesions (Ooshio et al., 2010; Zhang et al., 2011). Thus, we tested whether the relocation of ZO-1 to the plasma membrane following the activation of CaSR involved such an interaction between ZO-1 and I-afadin. First, confluent MDCK cells were exposed to LCM for 16 hours and then incubated in LCM supplemented with the type I CaSR agonists neomycin (1 mM) or Gd^{3+} (100 µM) for 30, 60 and 120 minutes (Fig. 5A,B). Cell lysates were subjected to immunoprecipitation using rabbit polyclonal antibodies directed against I-afadin, and the resultant immunoprecipitates were processed for immunoblotting using mouse monoclonal anti-ZO-1 antibodies. The total amounts of I-afadin and ZO-1 in cell lysates were also measured to ensure that equal quantities of these proteins were present under each condition. A faint interaction between I-afadin and ZO-1 could be detected in MDCK cells kept in LCM conditions. By contrast, the amount of ZO-1 protein that co-immunprecipitated with I-afadin was significantly increased after exposure to neomycin (Fig. 5A,B) or Gd^{3+} (data not shown), as early as 30 minutes following incubation. The level of interaction between I-afadin and ZO-1 did not significantly increase after 1 hour or 2 hours of continued incubation in comparison to the quantity detected at the 30 minute time point.

Next, confluent MDCK cells were exposed to a Ca^{2+} switch from 5 µM to 200 µM $[Ca^{2+}]_e$ in the presence of DMSO, R-568 or NPS-2143 (Fig. 5A,B). As previously reported (Zhang et al., 2011), the addition of Ca^{2+} to the culture medium induced the interaction between I-afadin and ZO-1. The co-immunoprecipitation of I-afadin and ZO-1 was significantly increased in the presence of the R-568 compound. Conversely, incubation of confluent MDCK cells with NPS-2143, partially blocked the interaction between I-afadin and ZO-1 induced by the Ca^{2+} switch to 200 µM $[Ca^{2+}]_e$.

Finally, MDCK cells initially kept in low-Ca^{2+} medium for 16 hours, were exposed to the AMPK activator AICAR (2 mM)

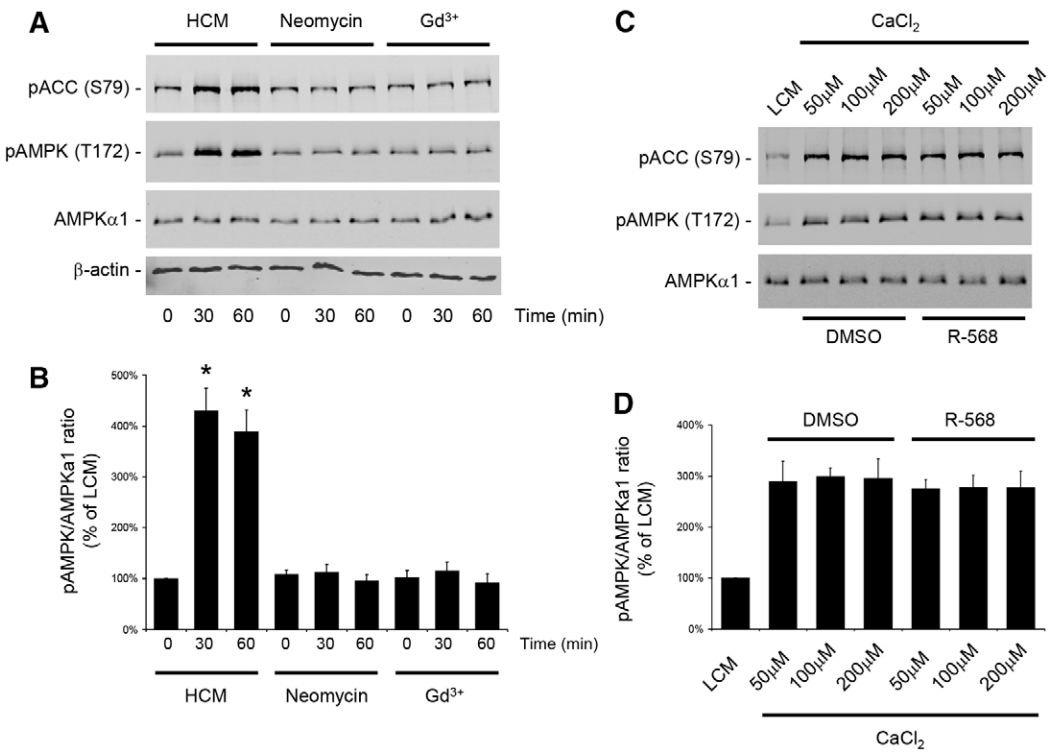

Fig. 4. CaSR activation does not stimulate AMPK phosphorylation or activation in MDCK cells. (A) Confluent MDCK cells were incubated in low-Ca^{2+} medium (LCM) for 16 hours, exposed to high-Ca^{2+} medium (HCM) or fresh LCM supplemented with the CaSR agonists neomycin (1 mM) or Gd^{3+} (100 μM) for 60 minutes, lysed in the presence of protease and phosphatase inhibitors, and probed with the indicated antibodies in a western blot analysis. (B) The quantification of the immunoreactive signal for phospho-AMPK was performed using the Odyssey Infrared Scanner (Li-Cor Biosciences) after normalization to the AMPKα1 expression level. Data represent mean percentages ± s.d., with the LCM level used as a reference (100%). *$P \leq 0.05$ versus LCM level by Student's *t*-test. (C) Confluent MDCK cells were incubated in LCM for 16 hours, exposed to fresh LCM supplemented with 50, 100 or 200 μM $CaCl_2$, with or without R-568 (800 nM) for 60 minutes, lysed in the presence of protease and phosphatase inhibitors and probed with the indicated antibodies in a western blot analysis. (D) The quantification of the immunoreactive signal for phospho-AMPK was performed as in B. No significant difference was observed between the lysates exposed to R-568 versus DMSO for any Ca^{2+} concentration.

and/or to the CaSR agonists R-568 (800 nM) and neomycin (1 mM), for 2 hours. Using a previously validated protocol (Zhang et al., 2006), we quantified relocation of ZO-1 to the plasma membrane following these different treatments. The length of ZO-1 deposits in MDCK cells stimulated by AICAR alone (11.4±1.7 μm/cell) or by AICAR and R-568 (10.2±2.1 μm/cell) or by AICAR and neomycin (12.2±2.4 μm/cell) was significantly higher than that measured in control MDCK cells kept in low-Ca^{2+} conditions (2.2±0.9 μm per cell), but not statistically different between treated groups (Fig. 5C,D). These observations suggest that both the CaSR and the AMPK cascades use a common final step in TJ assembly.

Pre-exposure of MDCK cells to BAPTA-AM prevents the relocation of TJ components to the plasma membrane induced by the stimulation of the CaSR, but does not affect TJ assembly induced by AMPK activation

The Ca^{2+} switch manipulation, which ultimately leads to TJ formation, is mediated primarily by Ca^{2+} acting at extracellular sites through the binding of Ca^{2+} to sites on E-cadherin extracellular repeats (Gonzalez-Mariscal et al., 1990; Contreras et al., 1992). In addition, changes in $[Ca^{2+}]_i$ have been detected both globally and in proximity to the sites of cell–cell contacts (Gonzalez-Mariscal et al., 1990; Contreras et al., 1992; Nigam et al., 1992). Chelation of Ca^{2+} by the Ca^{2+}-permeant chelator, bis-[2-aminophenoxy]-ethane tetraacetic acid [BAPTA-AM (50 μM)], significantly retards the relocation of ZO-1 to the plasma membrane produced by the Ca^{2+} switch (Stuart et al., 1994). To investigate whether the CaSR-related assembly of TJs requires free intracellular Ca^{2+}, we pre-exposed MDCK cells maintained in LCM for 16 hours to BAPTA-AM (50 μM) for 30 minutes before stimulating them with neomycin (1 mM) or R-568 (800 nM) for 2 hours. In control MDCK cells, ZO-1 was relocated to the plasma membrane following incubation with neomycin or R-568. In marked contrast, deposition of ZO-1 at the plasma membrane did not occur after similar incubations in MDCK cells that had first been exposed to BAPTA-AM (Fig. 6A,B). Furthermore, pre-exposure of MDCK cells to BAPTA-AM prevented the interaction between I-afadin and ZO-1 that is induced by stimulation of the CaSR with neomycin (Fig. 6C,D). Interestingly, the relocation of ZO-1 and its transient interaction with I-afadin, which are initiated by AMPK activation by AICAR (Zhang et al., 2011), were not significantly affected by pre-exposure of MDCK cells to BAPTA-AM (Fig. 6A–D). Moreover, the phosphorylation and activation of AMPK in MDCK cells following a Ca^{2+} switch was preserved in MDCK cells pre-exposed to BAPTA-AM (supplementary material Fig. S2).

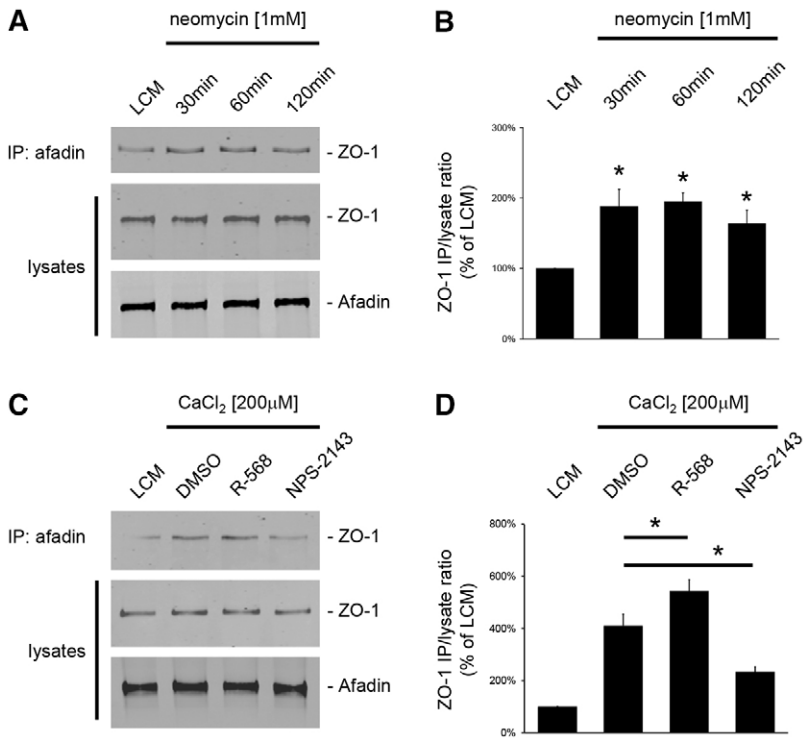

Fig. 5. Increased interaction between ZO-1 and I-afadin following activation of the CaSR in MDCK cells. (A) Confluent MDCK cells were incubated in low-Ca^{2+} medium (LCM) for 16 hours, exposed to fresh LCM supplemented with the CaSR agonist neomycin (1 mM) for the indicated time intervals, and lysed in presence of protease inhibitors. Cell lysates were immunoprecipitated using rabbit polyclonal antibodies directed against I-afadin and Protein-A agarose beads. Equal amounts of immunoprecipitates were then separated on SDS-PAGE and probed with mouse monoclonal anti-ZO-1 antibodies. Total cell lysates were simultaneously subjected to immunoblotting using anti-I-afadin and anti-ZO1 antibodies. (B) The quantification of the immunoreactive signal for ZO-1 in immunoprecipitates was performed using the Odyssey Infrared Scanner (Li-Cor Biosciences) and normalized to ZO-1 expression in total cell lysates. Data represent mean percentages ± s.d., with the LCM level used as a reference (100%). *$P \leq 0.05$ versus LCM level by Student's *t*-test. (C) Confluent MDCK cells were incubated in low-Ca^{2+} medium (LCM) for 16 hours, exposed to fresh LCM supplemented with 200 μM $CaCl_2$ and DMSO or the CaSR agonist R-568 (800 nM) or the CaSR antagonist NPS-2143 (1 μM) for 120 minutes and lysed in presence of protease inhibitors. Immunoprecipitation was performed as described in A. (D) The quantification of immunoreactive signals was performed as described in B. Data represent mean percentages ± s.d., with the LCM level used as a reference (100%). *$P \leq 0.05$ between indicated pairs using Student's *t*-test.

These observations suggest that free intracellular Ca^{2+} is required for the assembly of TJs that is induced by the stimulation of CaSR. By contrast, the relocation of ZO-1 caused by AMPK activation appears to be insensitive to the chelation of intracellular Ca^{2+}. These observations further support the conclusion that extracellular Ca^{2+} activates mechanistically distinct cascades that operate in parallel through the activation of the CaSR and the AMPK pathways to initiate TJ formation.

Stable expression of human disease-associated gain-of-function P221L CaSR mutant in MDCK cells increases TEER in comparison to MDCK cells expressing human wild-type CaSR

Mutations in the *CASR* gene have been associated with inherited disorders of divalent mineral homeostasis (Pearce et al., 1996). Gain-of-function mutations result in a downward resetting of the receptor EC_{50} and a leftward shift of the $[Ca^{2+}]_e$-response curve when compared with wild-type CaSR (Chattopadhyay and Brown, 2006; Letz et al., 2010; Hannan et al., 2012). In particular, the mutant Pro221Leu CaSR involves substitution of a non-polar residue for another non-polar residue in the extracellular domain, and has been associated with autosomal-dominant hypocalcemia with hypercalciuria (Conley et al., 2000; Letz et al., 2010). The stable transfection of a construct encoding a FLAG-tagged version of this human mutant CaSR in MDCK cells did not affect the distribution of the junction-associated protein, ZO-1, occludin and β-catenin, in comparison to MDCK cells expressing the wild-type form of human CaSR-FLAG. Still, the mutant Pro221Leu CaSR-FLAG was associated with a significantly and reproducibly higher TEER in comparison to the wild-type CaSR-FLAG (567.8±71.1 ohms.cm^2 versus 433.5±61.9 ohms.cm^2). Although variation of this magnitude could conceivably be caused by clonal variation, it is worth noting that the range of TEER difference observed between MDCK cells transfected with the wild-type versus the active form of the human CaSR corresponds to the range of TEER differences observed in confluent MDCK cells exposed to CaSR agonists diluted in normal-Ca^{2+} medium as compared to control conditions. Interestingly, wild-type CaSR-FLAG was found to be mostly located with β-catenin and the Na^+/K^+-ATPase (data not shown) at the basolateral membrane of MDCK cells (Fig. 7A). By contrast, the cellular distribution of P221L CaSR-FLAG included both the basolateral membrane and an intracellular compartment, suggesting that this mutant form of the receptor might manifest a defect in cellular trafficking (Fig. 7B). Moreover, wild-type CaSR-FLAG could be co-immunoprecipitated with β-catenin, whereas this interaction was partially lost in MDCK cells transfected with the active Pro221Leu mutant P221L (Fig. 7C). The electrophoretic mobility of the P221L mutant protein appeared to be different from that observed for the wild-type CaSR-FLAG protein in western blot analysis, with a reduction in the relative quantity of the 160-kD band corresponding to the fully glycosylated CaSR (Bai et al., 1996) (Fig. 7D). These observations suggested perturbations in the maturation state of N-linked glycosylation in the mutant or in the extent of other post-translational modifications. Deglycosylation studies using PGNase F and endo H enzymes revealed the absence of the endo-H-resistant mature form of the CaSR in cell lysates expressing the P221L mutant, in contrast to lysates expressing wild-type CaSR-FLAG (Fig. 7C, arrowhead). Taken together, these data show that the P221L mutation causes a defect in trafficking and maturation of the CaSR. This gain-of-function mutation is associated with an increased TEER of MDCK cells in comparison to wild-type CaSR, which further supports a role for the CaSR in TJ regulation.

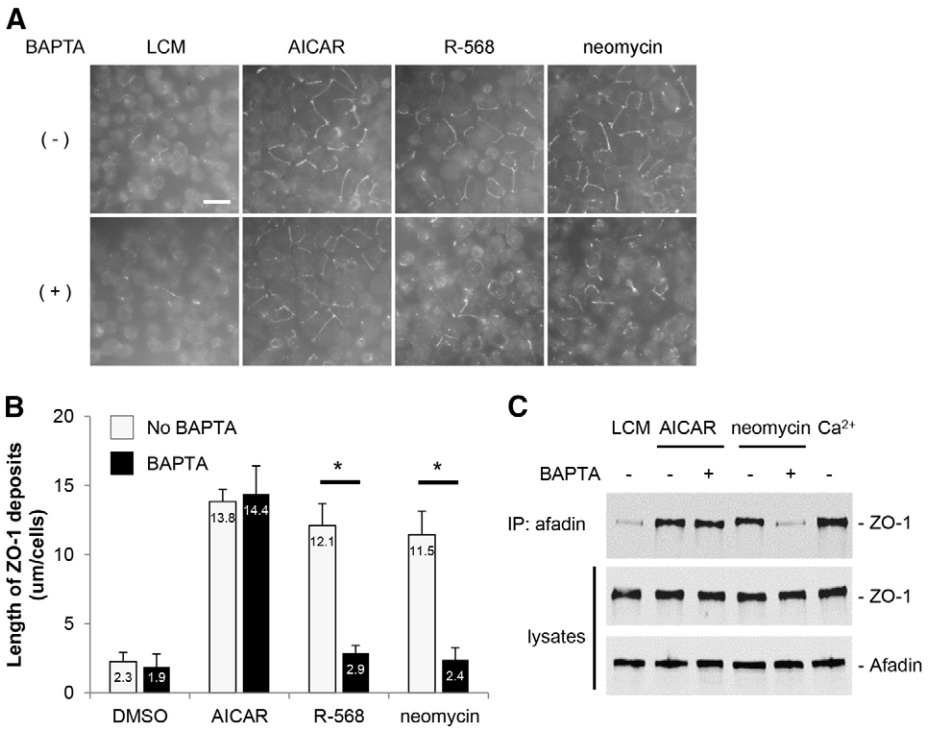

Fig. 6. Effects of the cell-permeant Ca^{2+} chelator, BAPTA-AM, on ZO-1 relocation to the plasma membrane after CaSR stimulation or AMPK activation in MDCK cells. (A) Confluent MDCK cells were incubated in low-Ca^{2+} medium (LCM) for 16 hours, exposed to fresh LCM supplemented or not with BAPTA-AM (50 μM) for 30 minutes, incubated with the CaSR agonists neomycin (1 mM) or R-568 (800 nM), or with the AMPK activator AICAR (1 mM) for 2 hours, fixed in ice-cold methanol and immunostained for ZO-1. Scale bar: 50 μm. (B) Quantification of ZO-1 relocation to cell membrane in A. Data represent means ± s.d. and are representative of three independent experiments. ZO-1 length per cell is measured within each of six randomly selected fields. *$P \leq 0.05$ between indicated pairs using Student's *t*-test. (C) Confluent MDCK cells were incubated in LCM for 16 hours, exposed to fresh LCM supplemented or not with BAPTA-AM (50 μM) for 30 minutes, incubated with the CaSR agonist neomycin (1 mM) or with the AMPK activator AICAR (1 mM) for 2 hours. Cells were lysed in the presence of protease inhibitors and immunoprecipitation was performed using rabbit polyclonal antibodies directed against I-afadin and Protein-A agarose beads. Equal amounts of immunoprecipitates were then separated on SDS-PAGE and probed with mouse monoclonal anti-ZO-1 antibodies. Total cell lysates were simultaneously subjected to immunoblotting using anti-I-afadin and anti-ZO1 antibodies. These data are representative of three independent experiments.

Discussion

Our present studies show that the activation of the CaSR in MDCK cells grown in low-Ca^{2+} conditions induces the relocation of TJ components to cell–cell contact sites, without significant changes in their mRNA expression. The CaSR is mainly located close to or at the basolateral membrane in MDCK cells, where it co-distributes with β-catenin. Its activation by well-established agonists such as neomycin and the calcimimetic compound R-568 causes a significant increase of TEER. In low-Ca^{2+} conditions, CaSR stimulation is associated with an increased interaction between I-afadin and ZO-1 and the relocation of TJ-associated proteins to the plasma membrane. These effects can be prevented by exposing the cells to (1) the CaSR antagonist NPS-2143, before Ca^{2+} switch or (2) to the cell-permeant Ca^{2+} chelator BAPTA-AM, before incubation with CaSR agonists. The activation of the CaSR in MDCK cells appears not to result in the phosphorylation or activation of AMPK. The stable expression of the human CaSR harboring the disease-associated gain-of-function P221L mutation causes a significant increase of TEER in comparison to MDCK cells transfected with a construct encoding the human wild-type CaSR.

The TJs form a dynamic intercellular seal that controls paracellular permeability and that participates in the regulation of a number of cellular processes including growth, differentiation and metabolism (Van Itallie and Anderson, 2004; Tsukita et al., 2008). TJs are composed of a complex assembly of integral and peripheral membrane proteins (Matter and Balda, 2003). Integral transmembrane protein components of TJs include claudins (CLDN), occludin and junction-associated molecule (JAM-A). As many as 40 peripheral proteins associate with the TJ and play crucial roles in their establishment and maintenance. The most important TJ adaptor proteins are members of the MAGUK (membrane-associated guanylate kinase) family, ZO-1, ZO-2 and ZO-3. ZO-1 and ZO-2 have essential roles in both organizing TJ components and targeting them to their proper location (Fanning and Anderson, 2009). In MDCK cells, the assembly of the TJ requires a transient interaction between ZO-1 and I-afadin, through the two proline-rich regions of I-afadin and the SH3 domain of ZO-1 (Yamamoto et al., 1997; Ooshio et al., 2010). During and after the formation of TJs, ZO-1 dissociates from I-afadin and associates instead with JAM-A. Here, we show that the pharmacological activation of the CaSR in the virtual absence of extracellular Ca^{2+} in MDCK cells is associated with (1) an increased interaction of ZO-1 with I-afadin, and (2) the relocation of ZO-1 and occludin to sites of cell–cell contact. These observations suggest that the recruitment of TJ components induced by CaSR stimulation bypasses the Ca^{2+}-dependent

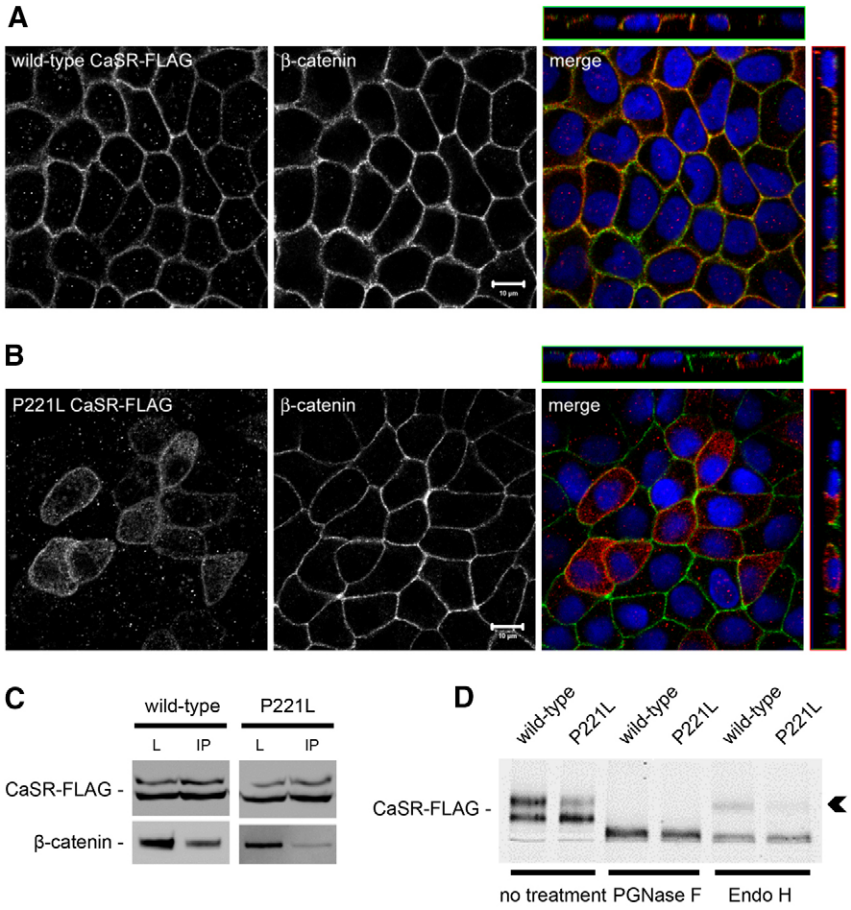

Fig. 7. Expression of human wild-type and the P221L active mutant of the CaSR in MDCK cells. (A,B) Representative co-immunofluorescence using rabbit polyclonal antibodies directed against FLAG and mouse monoclonal antibodies directed against β-catenin, a marker of the basolateral membrane, in MDCK cells stably transfected with wild-type human CaSR-FLAG (A) or with the human disease-associated P221L active mutant of the CaSR-FLAG (B). Merge panels show *xyz* planes, with the CaSR-FLAG labeled in red and β-catenin in green. Scale bars: 10 µm. (C) MDCK cells stably expressing human wild-type or P221L active mutant of the CaSR-FLAG were lysed in the presence of protease inhibitors and immunoprecipitated using mouse monoclonal antibodies directed against FLAG and protein-A agarose beads. Equal amounts of immunoprecipitates (IP) were then separated on SDS-PAGE and probed with rabbit polyclonal antibodies directed against β-catenin. Total cell lysates (L) were simultaneously subjected to immunoblotting using anti-FLAG and anti-β-catenin antibodies. These data are representative of three independent experiments. (D) MDCK cells stably expressing human wild-type or P221L active mutant of the CaSR-FLAG were lysed in the presence of protease inhibitors, incubated with the PGNase F and endo H deglycosylation enzymes for 60 minutes at 37℃, and probed with anti-FLAG antibodies in a western blot analysis. The arrowhead indicates the endo-H-resistant upper band of the CaSR-FLAG.

interactions between E-cadherin molecules of adjacent epithelial cells. This effect might be achieved by strengthening the trans interactions mediated by other cell adhesion molecules, such as those of the nectin–I-afadin system, and/or by modulating cytoskeleton dynamics near the cell membrane so that nascent cell–cell contacts are more stable, even without the participation of E-cadherin. It must be noted that the present data do not specifically demonstrate an effect on trans interactions. The CaSR-induced relocation of junction-associated proteins could be cell-autonomous and entirely independent of any change in intercellular interactions. In addition, although no significant changes in mRNA expression of TJ-associated proteins were observed following exposure to CaSR agonists, it remains unclear whether the activation of the CaSR is associated with exocytic delivery to or retention of TJ components at the plasma membrane.

The CaSR was first identified in tissues and cells implicated in Ca^{2+} homeostasis, including the parathyroid glands and the kidney (Brown et al., 1993; Tfelt-Hansen and Brown, 2005; Chakravarti et al., 2012; Geibel, 2010). Recent observations have demonstrated that the CaSR regulates the expression and distribution of members of the claudin (CLDN) family (Ikari et al., 2008; Gong et al., 2012). The expression of CLDN14 in epithelial cells lining the renal thick ascending limb is positively regulated by $[Ca^{2+}]_e$ through the CaSR (Gong et al., 2012; Dimke et al., 2013). Furthermore, the activation of the CaSR might decrease the PKA-mediated phosphorylation of CLDN16, thereby inducing its translocation and degradation in lysosomes (Ikari et al., 2008). These *in vitro* and *in vivo* observations emphasize the role of the CaSR in the regulation of TJ structure and function in cells implicated in Ca^{2+} homeostasis. Our results using cultured renal epithelial cells further support a role for the CaSR in the assembly of TJs. It is unlikely that this mechanism functions in all epithelial cells since the distribution of CaSR, although widespread, is not ubiquitous.

CaSR signaling is mediated through several heterotrimeric ($G_{q/11}$, $G_{i/o}$ and $G_{12/13}$) and small molecular weight G proteins that regulate intracellular second messengers, lipid and protein kinases, and transcription factors (Riccardi and Brown, 2012). The complexity of CaSR signaling is partly linked to the large variety of ligands that bind to the CaSR and to the diversity of cell types expressing this receptor. The best-characterized pathway involves the activation of phospholipase C by $G\alpha_{q/11}$, leading to the hydrolysis of phosphatidylinositol bisphosphate (PIP2) into diacylglycerol and IP3 and to a consequent increase in the intracellular Ca^{2+} concentration (Brennan and Conigrave, 2009). Both diacylglycerol and IP3-mediated elevations in $[Ca^{2+}]_i$ further activate the conventional protein kinase C pathway. In addition, the elevation in $[Ca^{2+}]_i$ can stimulate calmodulin-dependent processes, namely the stabilization of the CaSR at the plasma membrane by calmodulin itself and the activation of calmodulin-dependent protein kinase CaMKII. Alternatively, the CaSR-mediated activation of $G\alpha_{i/o}$ can also inhibit adenylate cyclase, thereby lowering intracellular cAMP levels (Geibel et al., 2006). Here, we found that exposure of MDCK cells to BAPTA-AM prevented the interaction of ZO-1

with I-afadin and its relocation to the plasma membrane following CaSR activation. These observations further support a role for $[Ca^{2+}]_i$ as the principle second messenger that mediates the influence of the CaSR on TJ assembly. By contrast, the pharmacological activation of AMPK by AICAR led to increased interaction between ZO-1 and I-afadin and TJ assembly, even in the presence of BAPTA. Furthermore, loading MDCK cells with BAPTA-AM did not affect the phosphorylation at Thr172 and the activation of AMPK during a Ca^{2+} switch. However, simultaneous activation of both the CaSR and the AMPK pathways in MDCK cells did not produce an additive effect on the extent of ZO-1 deposition at the plasma membrane in comparison to a solo stimulation of any of these pathways. Thus, these observations suggest that both the CaSR and the AMPK cascades use a common final step in TJ assembly. Additional studies are required to better identify the upstream cascade leading to AMPK activation during Ca^{2+}-induced TJ formation.

The EC_{50} value for Ca^{2+} binding at the CaSR in physiological conditions is 4.1 ± 0.1 mM $[Ca^{2+}]_e$ (Bai et al., 1996; Pearce et al., 1996), but can be significantly lowered by several physiological stimuli or by drugs such as R-568 (Hammerland et al., 1998; Petrel et al., 2004). Calcimimetics are positive allosteric modulators that bind in the transmembrane domain on the CaSR. In addition to its allosteric modulatory properties, the R-568 compound might also display partial agonism per se (Henley et al., 2011). Our studies show that switching MDCK cells from 5 μM to 50 μM $[Ca^{2+}]_e$ induces the relocation of ZO-1 to the plasma membrane. This was not prevented by pre-exposure to the CaSR antagonist, NPS-2143, but was significantly amplified by R-568. By contrast, the deposition of ZO-1 following a Ca^{2+} switch from 5 μM to 200 μM $[Ca^{2+}]_e$ was partially blocked by the CaSR antagonist, NPS-2143. Interestingly, we observed that AMPK was phosphorylated at Thr172 and activated during a Ca^{2+} switch from 5 μM to 50 μM $[Ca^{2+}]_e$, which could explain the CaSR-independent TJ assembly observed under these low-Ca^{2+} conditions. These observations further support the conclusion that multiple independent pathways manifesting distinct Ca^{2+} affinities are implicated in the Ca^{2+}-induced formation of TJs in epithelial cells.

Numerous observations support a pivotal role of the CaSR during the ontogeny of various organs and tissues, including the kidney, the lung, the gastro-intestinal tract, the nervous system and the bone (Riccardi and Kemp, 2012). During mouse development, CaSR immunoreactivity can be widely detected as early as embryonic day 11.5. In addition, plasma $[Ca^{2+}]$ levels in mammalian embryos are maintained above those in adults. The influence of biological factors, such as pH, oxygen availability and serum protein content, on the Ca^{2+} sensitivity of the CaSR *in utero* and at birth remains to be clarified. In differentiated tissues, such as the mucosa of the gastro-intestinal tract, the CaSR participates in the modulation of cell proliferation and differentiation (Ward et al., 2012). The human colonic epithelium, for example, manifests a rising $[Ca^{2+}]_e$ gradient from the base to the top of the crypt, which correlates with an increasing expression of the CaSR as epithelial cells migrate and differentiate towards the apex of the crypt. Such Ca^{2+} signaling mediated by the CaSR is thought to stop cell division, initiate cell differentiation, and favor E-cadherin-based junction formation to connect cells to one another (Chakrabarty et al., 2003). In colorectal carcinoma, epigenetic silencing of the *CASR* gene promoter by methylation is detected in 69% of cases and in 90% of lymph node metastases, correlating strongly with reduced CaSR expression (Hizaki et al., 2011). Taken together, these findings indicate that changes in $[Ca^{2+}]_e$ sensed by the CaSR participate in the regulation of TJ assembly or maintenance.

Mutations in the *CASR* gene have been associated with inherited disorders of divalent mineral homeostasis (Pearce et al., 1996; Hannan et al., 2012). Loss-of-function mutations in one or both of the *CASR* alleles result in hypercalcemic disorders, whereas gain-of-function mutations cause autosomal dominant hypocalcemia with hypercalciuria (ADHH) (Gunn and Gaffney, 2004; Thakker, 2004; Rus et al., 2008; Chattopadhyay and Brown, 2006, Letz et al., 2010). The gain-of-function mutation at nucleotide C662 (CCG to CTG) results in the substitution of a leucine residue for a proline residue in the extracellular bilobed Venus-fly-trap domain (VFTD) of the CaSR, which is predicted to contain five Ca^{2+}-binding sites (CaBSs) (Huang et al., 2007). The important role of the VFTD cleft has been recently illustrated by the identification and functional characterization of mutations involving codons 173 and 221, which code for residues that are located at the entrance to the VFTD cleft and lead to either a loss or a gain of CaSR function (Hannan et al., 2012). The activating Pro221Leu mutation is predicted to enhance the Ca^{2+} entry into CaBS-1 owing to the substitution of the rigid side chain of the wild-type proline residue at the entrance to the VFTD cleft with the more-flexible leucine side chain. Here, we show that the P221L mutation is associated with a defect in trafficking and maturation of the CaSR. In contrast to wild-type CaSR, which co-distributes with β-catenin at the basolateral membrane, the P221L mutant remains predominantly localized to intracellular compartments in MDCK cells. Furthermore, this mutant protein migrates in SDS-PAGE with an apparent molecular mass that is considerably smaller than that of the 160 kDa CaSR bearing fully mature N-linked glycosylation. The P221L protein is sensitive to deglycosylation by endoglycosydase H, suggesting that the bulk of the protein never leaves the endoplasmic reticulum nor does it undergo the Golgi-complex-associated maturation of its sugar chains. Interestingly, studies testing whether the calcilytic drug NPS-2143 could reduce the exaggerated signaling of activating mutants at physiological Ca^{2+} concentrations showed that the P221L mutant was sensitive to inhibition by this membrane-impermeant drug only when it is co-expressed with wild-type CaSR (Letz et al., 2010). Although these studies did not report on the subcellular distributions of the mutants, it is tempting to propose that co-expression of the wild-type form of the CaSR partially rescues the P221L trafficking defect and helps the mutant protein to reach the plasma membrane. If this was the case, then the effect of P221L mutation on CaSR function might not be attributable to changes in the affinity of the mutant receptor for extracellular Ca^{2+}. Rather, the mutation could exert its affect by trapping the receptor in the ER, thus leading to the continuous exposure of its extracellular domain to the very high Ca^{2+} concentrations that are present in the ER lumen. Thus, the apparent enhanced sensitivity of the P221L mutant receptor might instead reflect its constant exposure to a high Ca^{2+} environment. In MDCK cells, stable transfection of the human P221L mutant of the CaSR induces an increased TEER in comparison to cells expressing the human wild-type CaSR. These observations further support the role of the CaSR in the regulation of TJ properties.

In conclusion, our data demonstrate that the CaSR participates in the $[Ca^{2+}]_e$-induced assembly of TJs through an intracellular

mechanism that is dependent on $[Ca^{2+}]_i$. The activation of the CaSR in MDCK cells increases the interaction of ZO-1 with I-afadin and promotes recruitment of CaSR to the plasma membrane in the absence of AMPK phosphorylation and activation. Future studies will be required to determine the intracellular signaling cascade downstream of the CaSR that is responsible for TJ regulation.

Materials and Methods

Plasmids and constructs

C-terminally FLAG-tagged expression vectors (FLAG-N2) encoding wild-type and active mutant forms of the CaSR were generated by Dr Ch. Schöfl, Friedrich-Alexander University, Erlangen, Germany. Detailed information about these constructs was previously reported (Letz et al., 2010).

Cell culture and transfection

MDCK cells were maintained in α-MEM (Invitrogen) supplemented with 10% fetal bovine serum (Invitrogen), 2 mM L-glutamine (Invitrogen), 50 units/ml penicillin (Invitrogen) and 50 mg/ml streptomycin (Invitrogen). Cells were grown in a humidified incubator at 37℃ in a 5% CO_2 atmosphere. FLAG-N2 plasmids encoding human wild-type or P221L mutant CaSR sequences were transfected into MDCK cells by using Lipofectamine 2000 following the manufacturer's recommendations (Invitrogen). Selection and maintenance of stable MDCK cell clones were performed in α-MEM containing 1 mg/ml neomycin (Sigma). Clones were screened using rabbit polyclonal antibodies directed against FLAG by immunofluorescence (IF) and immunoblotting (IB) analyses.

Ca^{2+} switch and drug exposure experiments

MDCK cells were grown to confluence on plastic (for IB) or on coverslips (for IF) in α-MEM. Cells were then washed twice with minimum essential medium for suspension culture (S-MEM, Invitrogen) and incubated in S-MEM supplemented with 5% dialyzed fetal bovine serum, 2 mM L-glutamine, 50 units/ml penicillin and 50 mg/ml streptomycin (low-calcium medium, LCM). Cells were incubated in LCM for 16 hours before being switched back to α-MEM containing 1.8 mM Ca^{2+} (high-calcium medium, HCM) or exposed to drugs for the indicated times. Neomycin, gadolinium and bis-[2-aminophenoxy]-ethane tetraacetic acid (BAPTA-AM) were purchased from Sigma. Compound NPS-2143 was purchased from Tocris-Bioscience. Compound R-568 was obtained from Amgen (Thousand Oaks, CA). Final concentrations of DMSO never exceeded 0.1% (v/v).

Real-time RT-PCR

Total RNA was extracted from MDCK cells that had been exposed to different conditions using the Qiagen RNeasy kit, and reverse transcribed using SuperScript III reverse transcriptase (Invitrogen). Comparative mRNA expression analysis was performed by real-time RT-PCR (Agilent Technologies, Stratagene Mx3005P) using SYBR Green (QuantiTect, Qiagen), with glyceraldehyde-3-phosphate dehydrogenase (GAPDH) as the reference gene. The relative quantification of changes in target over GAPDH mRNA expression levels in comparison with baseline levels was performed using the $2^{\Delta\Delta Ct}$ formula (Pfaffl, 2001).

Antibodies

Rabbit anti-CaSR was from Millipore. Rabbit anti-pACC (Ser79), anti-α1-AMPK and anti-pAMPK (Thr172) were from Cell Signaling. Rabbit anti-β-catenin was from Santa Cruz Technology. Rabbit anti-I-afadin-I and anti-FLAG and mouse monoclonal anti-FLAG were from Sigma. Mouse monoclonal anti-ZO-1, anti-occludin and anti-β-actin were from Invitrogen, Zymed Laboratories and Abcam, respectively. Mouse monoclonal anti-Na^+/K^+-ATPase is directed against the N-terminus of rat α1 subunit (Tamkun and Fambrough, 1986). Rhodamine-conjugated goat anti-rabbit IgG was purchased from Chemicon. Alexa-Fluor-488-conjugated goat anti-mouse IgG and Alexa-Fluor-488-conjugated goat anti-rabbit IgG were purchased from Molecular Probes. Goat anti-mouse IRDye 800CW and anti-rabbit IRDye 680CW were purchased from Li-Core BioSciences. All commercially available antibodies were used according to the manufacturers' instructions.

Immunofluorescence and Quantification of ZO-1 Staining

Cells on coverslips were washed three times with cold PBS and fixed in 100% methanol at −20℃ for 10 minutes. Cells were then permeabilized in 0.3% Triton X-100, 0.15% BSA (permeabilization buffer) in PBS for 15 minutes at room temperature (RT) and blocked in goat serum dilution buffer (GSDB, 16% goat serum (Invitrogen), 20 mM sodium phosphate, pH 7.4, 450 mM NaCl, 0.3% Triton X-100) for 30 minutes at RT. Cells were incubated in primary antibody diluted 1:100 in GSDB for 1 hour at RT, after which they were immersed three times in permeabilization buffer, and then incubated for 1 hour in secondary antibody diluted 1:200 in GSDB at RT. Cells were then rinsed three times in PBS before mounting in Vectashield (Vector Laboratories). Cells were visualized on a Zeiss Axiophot fluorescence microscope equipped with a Zeiss AxioCamHRmCCDcamera, and on a Zeiss LSM 780 confocal laser-scanning microscope. Contrast and brightness settings were chosen so that all pixels were in the linear range. To quantify the mean ZO-1 length per cell, six fields were randomly selected from each coverslip, and the total length of ZO-1 at the cell periphery in each field was manually outlined, followed by length measurement with ImageJ software (National Institutes of Health). Pictures were taken in the focal plane in which the most strands of TJ components were visualized. Cell numbers were counted for each field by using propidium iodide (Molecular Probes) staining to reveal nuclei. Statistical analysis was performed using the two-tailed Student's *t*-test. In each case, the data presented are representative of at least three independent experimental repetitions.

Deglycosylation studies

Cell lysates from MDCK cells expressing either human wild-type FLAG-tagged CaSR or P221L mutant (20 µg protein/sample) were first exposed to denaturation buffer according to the manufacturer's recommendations (New England BioLabs) for 10 minutes at 50℃, incubated with deglycosylation enzymes, PGNase F or endo H, for 60 minutes at 37℃, and finally processed for western blotting analysis.

Co-immunoprecipitation and immunoblotting

Cells were lysed on ice in kinase lysis buffer (250 mM sucrose, 20 mM Tris-HCl, pH 7.4, 50 mM NaCl, 50 mM NaF, 5 mM sodium pyrophosphate, 1 mM Na3VO4, 2 mM fresh DTT, 1% Triton X-100) for 30 minutes, and sonicated for 15 seconds. Cell lysates were centrifuged at 15,000 rpm at 4℃ for 30 minutes, after which the supernatants were collected. Co-immunoprecipitation studies were performed using rabbit anti-I-afadin-I or mouse monoclonal anti-FLAG antibodies and Pierce Protein-A agarose beads (Thermo Scientific). Equal amounts of immunoprecipitates were resolved on an 8% SDS-polyacrylamide gel, and then electrophoretically transferred to 0.2 µm nitrocellulose membranes (Bio-Rad). Total cell lysates were also subjected to IB. Membranes were blocked with a milk solution (150 mM NaCl, 20 mM Tris-HCl, 5% milk (w/v), 0.1% Tween (v/v), pH 7.5) and successively probed with primary (diluted 1:1.000) and IRDye-conjugated secondary (diluted 1:10,000) antibodies diluted in a 5% BSA solution. Immunoreactive bands were detected using an Odyssey Infrared Scanner (Li-Cor Biosciences).

Acknowledgements

We thank all members of the Caplan laboratory for insightful advice and discussions.

Author contributions

XXXXX

Funding

This work was supported by the National Institutes of Health [grant numbers DK17433 and 072614]. F.J. is a Fellow of the Belgian American Educational Foundation and an MD Postdoctoral Fellow of the Fonds National de la Recherche Scientifique, and received support from a James Hudson Brown, Alexander Brown-Coxe Postdoctoral Fellowship (Yale University). Deposited in PMC for release after 12 months.

Supplementary material available online at
http://jcs.biologists.org/lookup/suppl/doi:10.1242/jcs.127555/-/DC1

References

Aberle, H., Butz, S., Stappert, J., Weissig, H., Kemler, R. and Hoschuetzky, H. (1994). Assembly of the cadherin-catenin complex in vitro with recombinant proteins. *J. Cell Sci.* **107**, 3655-3663.

Bai, M., Quinn, S., Trivedi, S., Kifor, O., Pearce, S. H., Pollak, M. R., Krapcho, K., Hebert, S. C. and Brown, E. M. (1996). Expression and characterization of inactivating and activating mutations in the human Ca^{2+}_o-sensing receptor. *J. Biol. Chem.* **271**, 19537-19545.

Balda, M. S., González-Mariscal, L., Contreras, R. G., Macias-Silva, M., Torres-Marquez, M. E., García-Sáinz, J. A. and Cereijido, M. (1991). Assembly and sealing of tight junctions: possible participation of G-proteins, phospholipase C, protein kinase C and calmodulin. *J. Membr. Biol.* **122**, 193-202.

Boller, K., Vestweber, D. and Kemler, R. (1985). Cell-adhesion molecule uvomorulin is localized in the intermediate junctions of adult intestinal epithelial cells. *J. Cell Biol.* **100**, 327-332.

Bräuner-Osborne, H., Wellendorph, P. and Jensen, A. A. (2007). Structure, pharmacology and therapeutic prospects of family C G-protein coupled receptors. *Curr. Drug Targets* **8**, 169-184.

Brennan, S. C. and Conigrave, A. D. (2009). Regulation of cellular signal transduction pathways by the extracellular calcium-sensing receptor. *Curr. Pharm. Biotechnol.* **10**, 270-281.

Brown, E. M., Gamba, G., Riccardi, D., Lombardi, M., Butters, R., Kifor, O., Sun, A., Hediger, M. A., Lytton, J. and Hebert, S. C. (1993). Cloning and characterization of an extracellular Ca(2+)-sensing receptor from bovine parathyroid. *Nature* **366**, 575-580.

Cereijido, M., Robbins, E. S., Dolan, W. J., Rotunno, C. A. and Sabatini, D. D. (1978). Polarized monolayers formed by epithelial cells on a permeable and translucent support. *J. Cell Biol.* **77**, 853-880.

Cereijido, M., Meza, I. and Martínez-Palomo, A. (1981). Occluding junctions in cultured epithelial monolayers. *Am. J. Physiol.* **240**, C96-C102.

Chakrabarty, S., Radjendirane, V., Appelman, H. and Varani, J. (2003). Extracellular calcium and calcium sensing receptor function in human colon carcinomas: promotion of E-cadherin expression and suppression of β-catenin/TCF activation. *Cancer Res.* **63**, 67-71.

Chakravarti, B., Chattopadhyay, N. and Brown, E. M. (2012). Signaling through the extracellular calcium-sensing receptor (CaSR). *Adv. Exp. Med. Biol.* **740**, 103-142.

Chang, W. and Shoback, D. (2004). Extracellular Ca2+-sensing receptors – an overview. *Cell Calcium* **35**, 183-196.

Chattopadhyay, N. and Brown, E. M. (2006). Role of calcium-sensing receptor in mineral ion metabolism and inherited disorders of calcium-sensing. *Mol. Genet. Metab.* **89**, 189-202.

Conley, Y. P., Finegold, D. N., Peters, D. G., Cook, J. S., Oppenheim, D. S. and Ferrell, R. E. (2000). Three novel activating mutations in the calcium-sensing receptor responsible for autosomal dominant hypocalcemia. *Mol. Genet. Metab.* **71**, 591-598.

Contreras, R. G., Miller, J. H., Zamora, M., González-Mariscal, L. and Cereijido, M. (1992). Interaction of calcium with plasma membrane of epithelial (MDCK) cells during junction formation. *Am. J. Physiol.* **263**, C313-C318.

Dimke, H., Desai, P., Borovac, J., Lau, A., Pan, W. and Alexander, R. T. (2013). Activation of the Ca(2+)-sensing receptor increases renal claudin-14 expression and urinary Ca(2+) excretion. *Am. J. Physiol.* **304**, F761-F769.

Fanning, A. S. and Anderson, J. M. (2009). Zonula occludens-1 and -2 are cytosolic scaffolds that regulate the assembly of cellular junctions. *Ann. N. Y. Acad. Sci.* **1165**, 113-120.

Fatherazi, S., Belton, C. M., Cai, S., Zarif, S., Goodwin, P. C., Lamont, R. J. and Izutsu, K. T. (2004). Calcium receptor message, expression and function decrease in differentiating keratinocytes. *Pflugers Arch.* **448**, 93-104.

Galli, P., Brenna, A., Camilli de, P. and Meldolesi, J. (1976). Extracellular calcium and the organization of tight junctions in pancreatic acinar cells. *Exp. Cell Res.* **99**, 178-183.

Gama, L., Baxendale-Cox, L. M. and Breitwieser, G. E. (1997). Ca^{2+}-sensing receptors in intestinal epithelium. *Am. J. Physiol.* **273**, C1168-C1175.

Geibel, J. P. (2010). The calcium-sensing receptor. *J. Nephrol.* **23 Suppl. 16**, S130-S135.

Geibel, J., Sritharan, K., Geibel, R., Geibel, P., Persing, J. S., Seeger, A., Roepke, T. K., Deichstetter, M., Prinz, C., Cheng, S. X. et al. (2006). Calcium-sensing receptor abrogates secretagogue- induced increases in intestinal net fluid secretion by enhancing cyclic nucleotide destruction. *Proc. Natl. Acad. Sci. USA* **103**, 9390-9397.

Gong, Y., Renigunta, V., Himmerkus, N., Zhang, J., Renigunta, A., Bleich, M. and Hou, J. (2012). Claudin-14 regulates renal Ca^{++} transport in response to CaSR signalling via a novel microRNA pathway. *EMBO J.* **31**, 1999-2012.

Gonzalez-Mariscal, L., Chávez de Ramírez, B. and Cereijido, M. (1985). Tight junction formation in cultured epithelial cells (MDCK). *J. Membr. Biol.* **86**, 113-125.

Gonzalez-Mariscal, L., Contreras, R. G., Bolívar, J. J., Ponce, A., Chávez De Ramirez, B. and Cereijido, M. (1990). Role of calcium in tight junction formation between epithelial cells. *Am. J. Physiol.* **259**, C978-C986.

Gumbiner, B. (1988). Cadherins: a family of Ca2+-dependent adhesion molecules. *Trends Biochem. Sci.* **13**, 75-76.

Gunn, I. R. and Gaffney, D. (2004). Clinical and laboratory features of calcium-sensing receptor disorders: a systematic review. *Ann. Clin. Biochem.* **41**, 441-458.

Hammerland, L. G., Garrett, J. E., Hung, B. C., Levinthal, C. and Nemeth, E. F. (1998). Allosteric activation of the Ca2+ receptor expressed in Xenopus laevis oocytes by NPS 467 or NPS 568. *Mol. Pharmacol.* **53**, 1083-1088.

Hannan, F. M., Nesbit, M. A., Zhang, C., Cranston, T., Curley, A. J., Harding, B., Fratter, C., Rust, N., Christie, P. T., Turner, J. J. et al. (2012). Identification of 70 calcium-sensing receptor mutations in hyper- and hypo-calcaemic patients: evidence for clustering of extracellular domain mutations at calcium-binding sites. *Hum. Mol. Genet.* **21**, 2768-2778.

Hardie, D. G. and Pan, D. A. (2002). Regulation of fatty acid synthesis and oxidation by the AMP-activated protein kinase. *Biochem. Soc. Trans.* **30**, 1064-1070.

Hays, R. M., Singer, B. and Malamed, S. (1965). The effect of calcium withdrawal on the structure and function of the toad bladder. *J. Cell Biol.* **25**, 195-209.

Henley, C., III, Yang, Y., Davis, J., Lu, J. Y., Morony, S., Fan, W., Florio, M., Sun, B., Shatzen, E., Pretorius, J. K. et al. (2011). Discovery of a calcimimetic with differential effects on parathyroid hormone and calcitonin secretion. *J. Pharmacol. Exp. Ther.* **337**, 681-691.

Hizaki, K., Yamamoto, H., Taniguchi, H., Adachi, Y., Nakazawa, M., Tanuma, T., Kato, N., Sukawa, Y., Sanchez, J. V., Suzuki, H. et al. (2011). Epigenetic inactivation of calcium-sensing receptor in colorectal carcinogenesis. *Mod. Pathol.* **24**, 876-884.

Huang, Y., Zhou, Y., Yang, W., Butters, R., Lee, H. W., Li, S., Castiblanco, A., Brown, E. M. and Yang, J. J. (2007). Identification and dissection of Ca(2+)-binding sites in the extracellular domain of Ca(2+)-sensing receptor. *J. Biol. Chem.* **282**, 19000-19010.

Ikari, A., Okude, C., Sawada, H., Sasaki, Y., Yamazaki, Y., Sugatani, J., Degawa, M. and Miwa, M. (2008). Activation of a polyvalent cation-sensing receptor decreases magnesium transport via claudin-16. *Biochim. Biophys. Acta* **1778**, 283-290.

Komuves, L., Oda, Y., Tu, C. L., Chang, W. H., Ho-Pao, C. L., Mauro, T. and Bikle, D. D. (2002). Epidermal expression of the full-length extracellular calcium-sensing receptor is required for normal keratinocyte differentiation. *J. Cell. Physiol.* **192**, 45-54.

Letz, S., Rus, R., Haag, C., Dörr, H. G., Schnabel, D., Möhlig, M., Schulze, E., Frank-Raue, K., Raue, F., Mayr, B. et al. (2010). Novel activating mutations of the calcium-sensing receptor: the calcilytic NPS-2143 mitigates excessive signal transduction of mutant receptors. *J. Clin. Endocrinol. Metab.* **95**, E229-E233.

Magno, A. L., Ward, B. K. and Ratajczak, T. (2011). The calcium-sensing receptor: a molecular perspective. *Endocr. Rev.* **32**, 3-30.

Martinez-Palomo, A., Meza, I., Beaty, G. and Cereijido, M. (1980). Experimental modulation of occluding junctions in a cultured transporting epithelium. *J. Cell Biol.* **87**, 736-745.

Matter, K. and Balda, M. S. (2003). Signalling to and from tight junctions. *Nat. Rev. Mol. Cell Biol.* **4**, 225-237.

Meldolesi, J., Castiglioni, G., Parma, R., Nassivera, N. and De Camilli, P. (1978). Ca++-dependent disassembly and reassembly of occluding junctions in guinea pig pancreatic acinar cells. Effect of drugs. *J. Cell Biol.* **79**, 156-172.

Nemeth, E. F. (2004). Calcimimetic and calcilytic drugs: just for parathyroid cells? *Cell Calcium* **35**, 283-289.

Nigam, S. K., Rodriguez-Boulan, E. and Silver, R. B. (1992). Changes in intracellular calcium during the development of epithelial polarity and junctions. *Proc. Natl. Acad. Sci. USA* **89**, 6162-6166.

Ooshio, T., Kobayashi, R., Ikeda, W., Miyata, M., Fukumoto, Y., Matsuzawa, N., Ogita, H. and Takai, Y. (2010). Involvement of the interaction of afadin with ZO-1 in the formation of tight junctions in Madin-Darby canine kidney cells. *J. Biol. Chem.* **285**, 5003-5012.

Palant, C. E., Duffey, M. E., Mookerjee, B. K., Ho, S. and Bentzel, C. J. (1983). Ca2+ regulation of tight-junction permeability and structure in Necturus gallbladder. *Am. J. Physiol.* **245**, C203-C212.

Pearce, S. H., Bai, M., Quinn, S. J., Kifor, O., Brown, E. M. and Thakker, R. V. (1996). Functional characterization of calcium-sensing receptor mutations expressed in human embryonic kidney cells. *J. Clin. Invest.* **98**, 1860-1866.

Petrel, C., Kessler, A., Dauban, P., Dodd, R. H., Rognan, D. and Ruat, M. (2004). Positive and negative allosteric modulators of the Ca2+-sensing receptor interact within overlapping but not identical binding sites in the transmembrane domain. *J. Biol. Chem.* **279**, 18990-18997.

Pfaffl, M. W. (2001). A new mathematical model for relative quantification in real-time RT-PCR. *Nucleic Acids Res.* **29**, e45.

Riccardi, D. and Brown, E. M. (2010). Physiology and pathophysiology of the calcium-sensing receptor in the kidney. *Am. J. Physiol.* **298**, F485-F499.

Riccardi, D. and Kemp, P. J. (2012). The calcium-sensing receptor beyond extracellular calcium homeostasis: conception, development, adult physiology, and disease. *Annu. Rev. Physiol.* **74**, 271-297.

Ringwald, M., Schuh, R., Vestweber, D., Eistetter, H., Lottspeich, F., Engel, J., Dölz, R., Jähnig, F., Epplen, J., Mayer, S. et al. (1987). The structure of cell adhesion molecule uvomorulin. Insights into the molecular mechanism of Ca2+-dependent cell adhesion. *EMBO J.* **6**, 3647-3653.

Rus, R., Haag, C., Bumke-Vogt, C., Bähr, V., Mayr, B., Möhlig, M., Schulze, E., Frank-Raue, K., Raue, F. and Schöfl, C. (2008). Novel inactivating mutations of the calcium-sensing receptor: the calcimimetic NPS R-568 improves signal transduction of mutant receptors. *J. Clin. Endocrinol. Metab.* **93**, 4797-4803.

Sedar, A. W. and Forte, J. G. (1964). Effects of calcium depletion on the junctional complex between oxyntic cells of gastric glands. *J. Cell Biol.* **22**, 173-188.

Stuart, R. O., Sun, A., Panichas, M., Hebert, S. C., Brenner, B. M. and Nigam, S. K. (1994). Critical role for intracellular calcium in tight junction biogenesis. *J. Cell. Physiol.* **159**, 423-433.

Tamkun, M. M. and Fambrough, D. M. (1986). The (Na+ + K+)-ATPase of chick sensory neurons. Studies on biosynthesis and intracellular transport. *J. Biol. Chem.* **261**, 1009-1019.

Tfelt-Hansen, J. and Brown, E. M. (2005). The calcium-sensing receptor in normal physiology and pathophysiology: a review. *Crit. Rev. Clin. Lab. Sci.* **42**, 35-70.

Thakker, R. V. (2004). Diseases associated with the extracellular calcium-sensing receptor. *Cell Calcium* **35**, 275-282.

Thomsen, A. R., Hvidtfeldt, M. and Bräuner-Osborne, H. (2012). Biased agonism of the calcium-sensing receptor. *Cell Calcium* **51**, 107-116.

Troy, T. C., Li, Y., O'Malley, L. and Turksen, K. (2007). The temporal and spatial expression of Claudins in epidermal development and the accelerated program of epidermal differentiation in K14-CaSR transgenic mice. *Gene Expr. Patterns* **7**, 423-430.

Tsukita, S., Yamazaki, Y., Katsuno, T., Tamura, A. and Tsukita, S. (2008). Tight junction-based epithelial microenvironment and cell proliferation. *Oncogene* **27**, 6930-6938.

Tu, C. L., Chang, W., Xie, Z. and Bikle, D. D. (2008). Inactivation of the calcium sensing receptor inhibits E-cadherin-mediated cell-cell adhesion and calcium-induced differentiation in human epidermal keratinocytes. *J. Biol. Chem.* **283**, 3519-3528.

Van Itallie, C. M. and Anderson, J. M. (2004). The molecular physiology of tight junction pores. *Physiology (Bethesda)* **19**, 331-338.

van Meer, G. and Simons, K. (1986). The function of tight junctions in maintaining differences in lipid composition between the apical and the basolateral cell surface domains of MDCK cells. *EMBO J.* **5**, 1455-1464.

Varani, J. (2011). Calcium, calcium-sensing receptor and growth control in the colonic mucosa. *Histol. Histopathol.* **26**, 769-779.

Ward, B. K., Magno, A. L., Walsh, J. P. and Ratajczak, T. (2012). The role of the calcium-sensing receptor in human disease. *Clin. Biochem.* **45**, 943-953.

Yamamoto, T., Harada, N., Kano, K., Taya, S., Canaani, E., Matsuura, Y., Mizoguchi, A., Ide, C. and Kaibuchi, K. (1997). The Ras target AF-6 interacts with ZO-1 and serves as a peripheral component of tight junctions in epithelial cells. *J. Cell Biol.* **139**, 785-795.

Zhang, L., Li, J., Young, L. H. and Caplan, M. J. (2006). AMP-activated protein kinase regulates the assembly of epithelial tight junctions. *Proc. Natl. Acad. Sci. USA* **103**, 17272-17277.

Zhang, L., Jouret, F., Rinehart, J., Sfakianos, J., Mellman, I., Lifton, R. P., Young, L. H. and Caplan, M. J. (2011). AMP-activated protein kinase (AMPK) activation and glycogen synthase kinase-3β (GSK-3β) inhibition induce Ca^{2+}-independent deposition of tight junction components at the plasma membrane. *J. Biol. Chem.* **286**, 16879-16890.

Zheng, B. and Cantley, L. C. (2007). Regulation of epithelial tight junction assembly and disassembly by AMP-activated protein kinase. *Proc. Natl. Acad. Sci. USA* **104**, 819-822.